수직-수평 반복하중을 받는 알루미나 표면에서의 피로손상 누적

이 권 용, 최 성 종
대구대학교 자동차 · 산업공학부

Surface damage accumulation in alumina under the repeated inclined contact forces

Kwon-Yong Lee, Sung-Jong Choi
School of Automobile, Industrial, and Mechanical Engineering, Taegu University

Abstract

반복 응력 상태 아래서 알루미나 세라믹의 피로 표면손상 누적현상이 분석되었다. 연속 미끄럼 접촉 시에 발생하는 응력 상태를 재현하기 위해서 동시에 작용하는 수직-수평 반복 압축하중 기법이 사용되었다. 알루미나 구와 평판의 접촉면에서 알루미나 미세 결정의 피로 파손에 의한 마모 입자 형성 기구가 관찰되었고, 반복하중의 횟수와 수직-수평 하중비가 커질수록 마모량은 증가하였다. 반복 접촉하중에 의한 표면손상 누적이 접촉 수직 변위 측정으로 정량화 되었다. 두 접촉 구조물의 강성 (하중-변위 선도의 기울기) 변화가 두 재질의 탄성계수의 변화로 표현되었다.

Keywords: synchronized biaxial repeated indentation, fatigue wear mode, surface damage accumulation, alumina.

1. Introduction

Early studies on the wear of ceramic materials classified the wear mechanisms in terms of conventional phenomenological expressions: abrasive, adhesive, erosive, and corrosive wear, etc. In recent times, more fundamental modes: brittle fracture, plastic deformation, and fatigue, have been suggested. When two ceramic surfaces are brought into sliding contact, they inflict mutual damage on each other, resulting in loss of material. This material removal essentially involves the fracture process where the crack nucleation and propagation will depend on the loading history and environment.

Although it has always been generally believed that ceramics materials are not susceptible to fatigue degradation under cyclic stress state since they have limited crack-tip plasticity, there exist conventional tension/compression fatigue data indicating that fatigue effect may be possible in wear process in alumina ceramics [1, 2]. Lathabai et al. [3] and Cho et al. [4] showed the effect of microstructure, especially, grain size on the fatigue cracking and wear of alumina. And also Ajayi et al. [5] suggested that surface fatigue may be responsible for the micro-damage wear mechanism having an incubation period; after this period wear

rate increased.

It is clear that any point below the sliding track experiences a cyclic stress history as the contact region moves along the surface repeatedly. The fatigue can occur under the repeating combined shear-compressive and shear-tensile stresses. These cyclic stresses will induce accumulation of surface damage and cause time-dependent (cycle-dependent) failures.

Recently, a simple technique based on repeated indentation with a sharp indenter has been proposed as a method for studying cyclic fatigue effects in ceramics [6]. Lu et al. [7] conducted indentations with a sphere instead of a sharp diamond indenter to analyze the damage induced by cyclic tangential loading of contacting elastic bodies. Guiberteau et al. [8] tested the indentation fatigue with a simple Hertzian contact producing the culmulative mechanical damage on ceramic surfaces. But the stress states under above cases are clearly different from the case of repeat pass sliding.

In this work, the normal and tangential load were applied and released simultaneously to achieve a stress sequence on a point of sliding wear track. For ball on flat contact under this alternating stress, not only the mode of material removal will be analyzed , but the surface degradation due to fatigue cracking accumulating also be quantified by measuring contact displacement.

2. Method

Alumina-based ceramic cutting tool inserts (84% alumina, 12% zirconia, and 3% titanium diboride, 12.7 x 12.7 x 47.5mm, GTE Valenite Crop.) were used for the flat specimens and 99.5% alumina oxide (diameter of 6.35mm, Industrial Tectonics Inc.) were used for the ball specimens. Some mechanical properties of ball and flat specimens are listed in Table 1.

Table 1 Material properties of the ball and flat specimens.

Material Property	Ball	Flat
Young's Modules (GPa)	370	400
Poisson's Ratio	0.23	0.24
Vickers Hardness (Kg/mm^2)	1400	1800
Fracture Toughness (AN/m^3)	3.2	3.0
Density (g/cm^3)	3.86	4.2
Grain Size (μm)	7.0±4.0	2.0±1.0

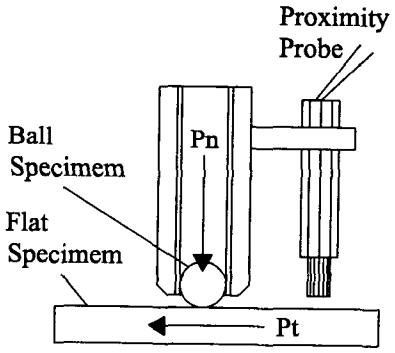

Figure 1. Schematic diagram of the cyclic fatigue indentation device

Synchronized biaxial repeated indentions were performed using the newly designed machine, named Cyclic Fatigue Indentation Device. Figure 1 shows a schematic diagram of the test machine. The normal and tangential loads were applied through connecting steel cables by two air cylinders, respectively. The load amplitude were controlled with signals from strain gages attached on the loading bars. The working

pressure of air cylinders is controlled by the electro-pneumatic pressure regulator whose electric input was generated in an isosceles triangular wave by a computer. A MicroProx proximity probe was mounted on a ball holder and placed with a proper initial gap at a right angle against the top surface of the flat specimen holder. Indentation load data and contact displacement data were stored with a multi-channel scan data acquisition program in a computer.

The surface of the flat specimens were ground by SiC disc papers and then polished with diamond paste. The measured arithmetic average roughness heights, R_a, of flat specimens are 0.05μm. The ball specimens were used as-received; the manufacturer quotes the roughness of the balls as 0.04μm.

Four peak normal contact loads, 480N, 530N, 590N, 730N, were applied. The lowest load for cone crack formation in a fully elastic brittle fracture theory with a single indentation [9]. Four peak synchronized tangential loads were applied for each normal load according to load ratios ($L=P_t/P_n$) of 0.0, 0.05, 0.14, and 0.23. The tangential force is limited far below the static coefficient of friction value of 0.5.

All tests were conducted in air using a frequency of 0.04Hz. The number of cycles ranged up to 960 cycles. These test conditions were determined from preliminary tests to produce definitive surface damage. After tests, the contact surface damage was examined with optical and scanning electron microscopes.

3. Results

In repeated indention tests, though no sliding occurred, two kinds of surface damage were observed. At first, the material removal in micro-scale of grain size level or less was observed within the contact area, and at high contact stress, macro-scale (ring/horse shoe) cracks were also seen near the contact edge (Figure 2.a).

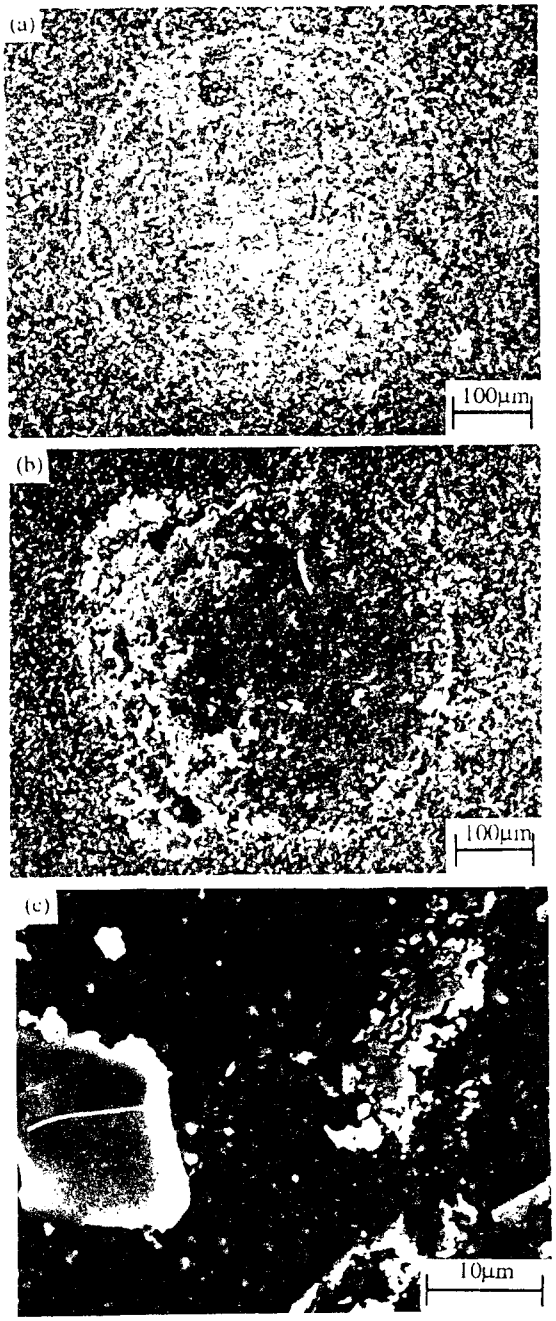

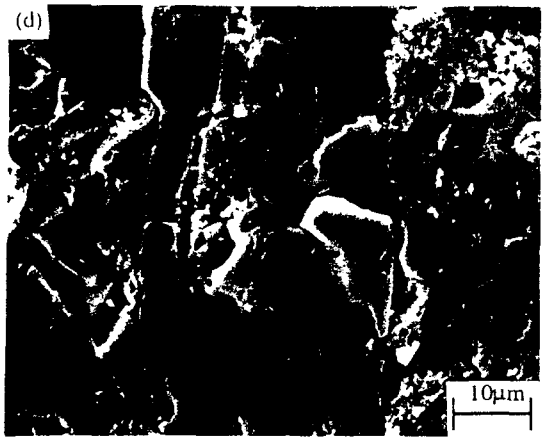

Figure. SEM photos showing the contact damage of debris and cracks with (a) 730N, (b) 730N and L=0.23, (c) 480N on the flat specimen, and (d) 730N and L=0.23 on the ball specimen after 960 indentation cycles.

Under low combined load, micro-scale wear occurred without visible macro-cracks. As the applied loads increases, the area covered with debris spread over the contact region. An additional horizontal traction remarkably increases the amount of debris (Figure 2.b). These damage accumulated through fatigue as the number of indentation increased.

The size of debris at the early stage under the lowest load is uniform and about 3μm. As the number of indentation and applied normal load increase, large debris over 10μm size were generated the grain failure and some of them are crushed (Figure 2.c). This result supports that the actual wear occurs vis a fatigue mode on a micro-scale by grain failure; the removed grains subsequently are fragmented in a brittle mode under repeated loading.

Surface degradation due to contact damage accumulation was detected by the change of slope in contact load-displacement curves (hysteresis loops). Under a low normal indentation load of 480N, there was little change in each hysteresis loops which is very close to a theoretical elastic Herzian contact curve. After the macro-crack formed under the given load combination, the change of slope became large. Under the severe load combination of 730N and L=0.23, broadening of loop between the loading and unloading paths as well as a very large decrease in slope occurred (Figure 3). This pattern was accompanied with the series of macro-crack formation and the following large micro-scale wear debris pile-up. This slope change of hysteresis as the number of indentation increased.

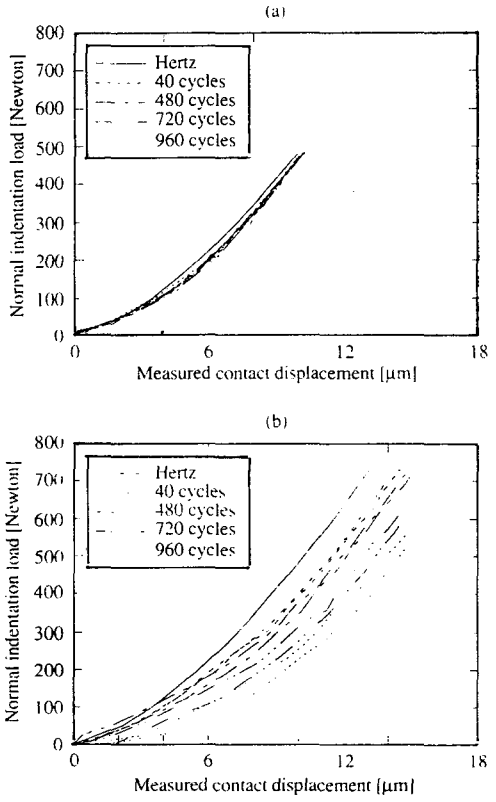

Figure 3. Variation of hysteresis loops with (a) 480N and (b) 730N and L=0.23.

4. Discussions

Energy dispersive X-ray analysis showed that most debris on the flat specimens originated from the ball surfaces. Figure 2.d shows the debris detached from a ball. The flat specimen and ball specimen have different composition and surface finish. In the viewpoint of microstructure, the biggest difference between them seems to be the grain size. The nominal grain size is 1-3μm for a flat specimen and 3-11μm for a ball. The result that coarser grain structure of ball is more susceptible to micro-scale material removal via grain boundary failure than fine structure of flat specimens agree well with the other results [4, 10, 11].

There is a noticeable increase of contact displacement with increasing load ratio (coefficient of friction) due to formation of macro-crack. The addition of the horizontal traction increases the crack driving force with increased tensile stresses near the trailing edge, aggravates the surface damage, and makes the hysteresis loop decline. The gap between loading and unloading paths may arise from the additional fracture during the unloading process. The possible mechanism of crack growth during unloading is crack tip opening with wedge action of existing particles on the crack faces under reverse loading [2].

As the first step for quantifying the degree of surface damage accumulation, a trial is made to correlate the variation of measured contact displacement with the change of apparent elastic constant. Provided all assumptions of Hertzian contact are retained on each cycle, apparent radius of curvature R is fixed and applied load P is known. Therefore, the variation of measured contact displacement enables an approximation of the change in apparent elastics constant E* of the contact system during repeated indentation. It can be expressed in the following simple formula from Hertzian theory [12].

$$E^* = \left| \frac{9\,P^2}{16\,R\,\delta^3} \right|^{1/2}$$

But, because contact failure may occur within a localized thin layer and because the stiffness decrease is not a change of bulk elastic property, the apparent elastic constant calculated from above equation will be called the "pseudo elastic constant" (E*)'. The variation of pseudo elastic constant (E*)' at each peak load are plotted in Figure 4 according to the number of indentation cycles.

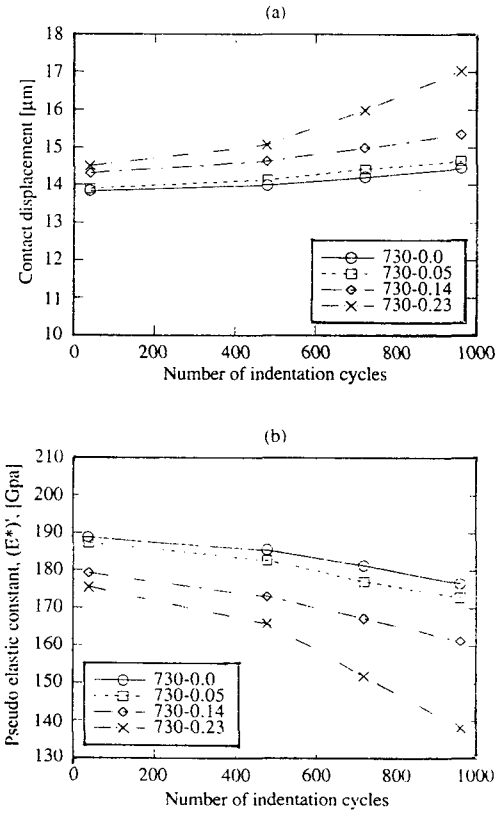

Figure 4. Variation of the (a) contact displacement and (b) elastic constant of contact system with 730N and each load ratio.

5. Conclusion

Under the synchronized cyclic normal and tangential loads the actual wear occurs in a fatigue mode by grain failure and micro fragmentation at the contact interface. Fatigue wear mode was confirmed by the increase of material removal rate as the number of cycles increases in connection with increase of load ratio.

Surface fatigue degradation resulting from the progression of fatigue failure under synchronized cyclic normal and tangential loading was quantified by the increase of compliance in contact system which is expressed as a variation of the apparent elastic properties of the contacting bodies within a localized thin contact layer. Test methodology used in this research could be used to indicate the structural integrity of ceramic surfaces.

Reference

1. Ewart, L.E. and Suresh, S., "Crack Propagation in Ceramics under Cyclic Loads," J. Master. Sci., Vol.22 [4], pp.1173-1192, 1987.

2. Reece, M.J., Guiu, F., and Sammur, M.F.R., "Cyclic Fatigue Crack Propagation in Alumina under Direct Tension-Compression Loading," J. Am. Ceram. Soc., 72 [2], pp.348-352, 1989.

3. Lathabai, S., Rödel, J., and Lawn, B.R., "Cyclic Fatigue from Frictional Degradation at Bridging Grains in Alumina," J. Am. Ceram. Soc., 74 [6], pp.1340-1348, 1991.

4. Cho, S.J., Hockey, B.J., lawn, B.R., and Bennison, S.J., "Grain Size and R-Curve Effects in the Abrasive Wear of Alumina," J.Am. Ceram. Soc., Vol.72 [7], pp.1249-1252, 1989.

5. Ajayi, O.O. and Ludema, K.C., "Surface Damage of Structural Ceramics: Implications for Wear Modeling," Wear, Vol. 124, pp.237-257, 1988.

6. Reece, M. and Guiu, F., "Repeated Indentation Method for Studying Cyclic Fatigue in Ceramics," J. Am. Ceram. Soc., 73 [4], pp.1004-1013, 1990.

7. Lu, M.C. and Evans, A.G., "Influence of Cyclic Tangential Loads on Indentation Fracture." J. Am. Ceram. Soc., 68 [9], pp.505-510, 1985.

8. Guiberteau, F., Padture, N,P., Cai, H., and Lawn, B.R., "Indentation Fatigue A Simple Cyclic Hertzian Test for Measuring Damage Accumulation in Polycrystalline Ceramics," Philosophical Magazine A, Vol. 68 [5], pp.1003-1016, 1993.

9. Mouginot, R. and Maugis, D., "Fracture Indentation beneath Flat and Spherical Pumches," J.Mater. Sci., Vol. 20, pp.4354-4376, 1985.

10. Lawn, B.R., Freiman, S.W., Baker, T.L., Cobb, D.D., and Gonzalez, A.C., "Study of Alumina Using Controlled Flaws," J. Am. Ceram. Soc., Vol. 67 [4], pp.c-67-c-69, 1984.

11. Wang, Y.S., He, c., Hockey, B.J., Lacey, P.I., and Hsu S.M., "Wear Transitions in Monelithic Alumina and Zirconia-Alumina Composites," Wear, Vol. 181-183, pp.156-164, 1995.

12. JOhnson, K.L., "Contact Mechanics," Cambridge University Press, Cambridge, pp84-106, 1985.